

# Reversible Photoresponsive Chiral Liquid Crystals Containing a Cholesteryl Moiety and Azobenzene Linker

Quan Li,\* Lanfang Li, Julie Kim, Heung-shik Park, and Jarrod Williams

Liquid Crystal Institute, Kent State University, Kent, Ohio 44242

Received June 28, 2005. Revised Manuscript Received September 29, 2005

Two new chiral liquid crystals containing a well-known mesogenic cholesteryl group and an azobenzene moiety connected with a short flexible carbonyldioxy spacer and a polar carbonyl unit in a terminal chain were designed and synthesized. A sequence of very interesting mesophases were observed. Their reversible photoresponsive properties were well-demonstrated by UV irradiation. The two materials as chiral mesogenic dye dopants have a very large solubility in a common nematic liquid crystal host, which can facilitate a large amount of doping to induce mesophase chirality and magnify the photocontrolling effect.

## Introduction

Liquid crystals containing an azo linkage, either low molar mass or polymeric in nature, have attracted tremendous attention as a result of their unique photoswitchable properties induced by light.<sup>1–6</sup> *trans*-Azobenzene is thermodynamically more stable than *cis*-azobenzene by about 56 kJ/mol; however, irradiation with ultraviolet light of wavelength of about 360 nm leads to reversible *trans*–*cis* isomerization. The reverse process from the *cis* to the *trans* isomer can occur thermally or photochemically with visible light.<sup>7–10</sup> Because the physical and chemical properties of the two azobenzene configurational isomers are different, the reversible optically induced switching effect has been the basis for many functional molecules and materials with applications in optical switching, liquid crystal display, holography, and data storage in various media.<sup>11</sup> For example, a polarizer with better reflectance can usually be achieved by dissolving a nonmesogenic azo compound in liquid crystals. Azo molecules are also used in low power consumption reflective liquid crystal devices because of their pronounced dichroic ratio.<sup>12</sup> A combination of nonmesogenic azo compounds with chiral nematic (cholesteric) liquid crystals has been demonstrated as a replacement for the polarizer in display devices.<sup>13</sup>

However, the addition of nonmesogenic azo molecules often causes instability of the liquid crystalline phase. Few developments of chiral liquid crystals with azo linkage were reported to date,<sup>14–15</sup> compared with numerous nonmesogenic azo dyes and some achiral azo liquid crystals.<sup>16,17</sup> To tailor azo compounds with chiral mesogenic properties, here we report the design and synthesis of two photoresponsive chiral liquid crystals **3a** and **3b** containing a well-known mesogenic cholesteryl group and an azobenzene moiety connected with a short flexible carbonyldioxy spacer and a polar carbonyl unit in a terminal chain. To the best of our knowledge, these are the first two compounds with the general structure **3** (Scheme 1) to be synthesized. The interest behind the design of the new photoresponsive chiral liquid crystals with the cholesteryl group mainly results from the rigid long shape, chiral structure, and distinct optical properties of the cholesteryl group. The rigid long shape can induce anisotropic intermolecular interaction via van der Waals forces which can stabilize parallel molecular stacking, and the chiral structure of the cholesteryl group can induce chirality in molecular order, namely, helical superstructure.<sup>18</sup> Meanwhile, the introduction of a polar carbonyl unit into a terminal chain can aid the lateral attraction between molecules and generate a strong smectic character.<sup>19</sup>

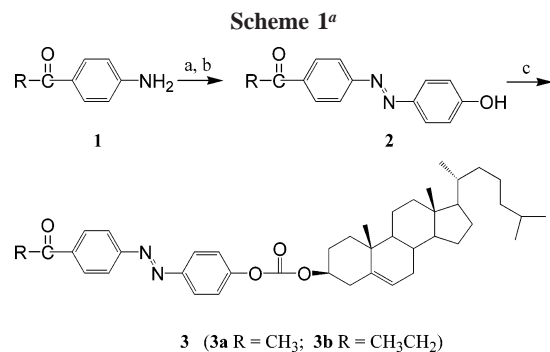
\* To whom correspondence should be addressed. Tel.: 1-330-672-1537. Fax: 1-330-672-2796. E-mail: quan@lci.kent.edu.

- (1) Ruslim, C.; Ichimura, K. *J. Mater. Chem.* **1999**, *9*, 673.
- (2) Urbas, A.; Tondiglia, V.; Natarajan, L.; Sutherland, R.; Yu, H.; Li, J.-H.; Bunning, T. *J. Am. Chem. Soc.* **2004**, *126*, 13580.
- (3) Ichimura, K.; Oh, S.-K.; Nakagawa, M. *Science* **2000**, *288*, 1624.
- (4) Komitov, L.; Ichimura, K.; Strigazzi, A. *Liq. Cryst.* **2000**, *27*, 51.
- (5) Komitov, L.; Ruslim, C.; Matsuzawa, Y.; Ichimura, K. *Liq. Cryst.* **2000**, *27*, 1011.
- (6) Ikeda, T.; Tsutsumi, O. *Science* **1995**, *268*, 1873.
- (7) Holme, N. C. R.; Ramanujam, P. S.; Hvilsted, S. *Opt. Lett.* **1996**, *21*, 902.
- (8) Ikeda, T.; Horiuchi, S.; Karanjit, D. B.; Kurihara, S.; Tazuke, S. *Macromolecules* **1990**, *23*, 36.
- (9) Janossy, I.; Szabados, L. *J. Nonlinear Opt. Phys. Mater.* **1998**, *7*, 539.
- (10) Yu, Y.; Nakano, M.; Ikeda, T. *Nature* **2003**, *425*, 145.
- (11) Ikeda, T. *J. Mater. Chem.* **2003**, *13*, 2037.
- (12) Sunohara, K.; Naito, K.; Tanaka, M.; Naikai, Y.; Kamiura, N.; Taira, K. *SIDDIG* **1996**, *103*.
- (13) Tanaka, M. *Flat Panel Disp. Intelligence* **1997**, *4*, 70.

## Experimental Section

**Materials and Methods.** All chemicals and solvents were purchased from commercial suppliers and used without further

- (14) Lee, H.-K.; Doi, K.; Harada, H.; Tsutsumi, O.; Kanazawa, A.; Shiono, T.; Ikeda, T. *J. Phys. Chem. B* **2002**, *104*, 7023.
- (15) Tong, X.; Zhao, Y. *J. Mater. Chem.* **2003**, *13*, 1495.
- (16) Jakli, A.; Prasad, V.; Shankar Rao, D. S.; Liao, G.; Jánossy, I. *Phys. Rev. E* **2005**, *71*, 021709.
- (17) Prasad, V.; Kang, S.-W.; Qi, X.; Kumar, S. *J. Mater. Chem.* **2004**, *14*, 1459.
- (18) (a) Janicki, S. Z.; Schuster, G. B. *J. Am. Chem. Soc.* **1995**, *117*, 8524. (b) Denekamp, C.; Feringa, B. L. *Adv. Mater.* **1998**, *10*, 1080.
- (19) Collings, P. J.; Hird, M. In *Introduction to Liquid Crystals: Chemistry and Physics*; Gray, G. W., Goodby, J. W., Fukuda, A., Eds.; Taylor & Francis, Ltd.: London, 1997.



<sup>a</sup> (a) NaNO<sub>2</sub>, aqueous HCl; (b) phenol; (c) cholesteryl chloroformate.

purification. Melting points are uncorrected. <sup>1</sup>H and <sup>13</sup>C NMR spectra were recorded in CDCl<sub>3</sub>. Chemical shifts are in δ units (ppm) with the residual solvent peak (<sup>1</sup>H CHCl<sub>3</sub>, δ 7.26; <sup>13</sup>C CDCl<sub>3</sub>, δ 77) as the internal standard. The coupling constant (*J*) is reported in hertz (Hz). NMR splitting patterns are designated as s, singlet; d, doublet; t, triplet; q, quartet; and m, multiplet. Column chromatography was carried out on silica gel (60–200 mesh). Analytical TLC was performed on commercially coated 60 mesh F<sub>254</sub> glass plates. Spots were rendered visible by exposing the plate to UV light. Infrared spectra were recorded using a Nicolet Fourier transform infrared spectrometer with a KBr pellet. The UV irradiation was carried out by a 10 mW/cm<sup>2</sup> UV lamp with a 365 nm peak wavelength. Textures and transition temperatures for target compounds were observed by optical microscopy using a Leitz polarizing microscope in conjunction with a Linkam TMS temperature controller. Calorimetric measurements were performed in a Perkin-Elmer differential scanning calorimeter (DSC) using indium and zinc as standards for calibration.

**Synthesis.** Photoresponsive chiral liquid crystals **3a** and **3b** were synthesized starting from 4-substituted aniline **1** which was reacted with sodium nitrite in aqueous HCl to give diazonium salt followed by coupling with phenol to obtain azo intermediate **2**. The azo intermediate **2** was treated with cholesteryl chloroformate to afford azo **3** as orange or reddish orange crystals with a high yield (Scheme 1). Their structures were identified by <sup>1</sup>H NMR, <sup>13</sup>C NMR, and IR.

**Data for 3a.** Mp 179 °C; IR (KBr)  $\nu_{\max}$  (cm<sup>-1</sup>) 2936, 2867, 1761, 1685, 1653, 1598, 1498, 1466, 1414, 1357, 1268, 1225, 1141, 1106, 1050, 1008, 972, 853; <sup>1</sup>H NMR (δ, CDCl<sub>3</sub>) 8.11 (d, *J* = 8.8 Hz, 2H), 8.00 (d, *J* = 7.2 Hz, 2H), 7.96 (d, *J* = 7.2 Hz, 2H), 7.38 (d, *J* = 8.8 Hz, 2H), 5.44 (d, *J* = 4.8 Hz, 1H), 4.62 (m, 1H), 2.67 (s, 3H), 2.51 (d, *J* = 7.2 Hz, 2H), 0.89–2.06 (m, 38H), 0.69 (s, 3H); <sup>13</sup>C (δ, CDCl<sub>3</sub>) 197.44, 154.89, 153.54, 152.43, 150.10, 139.01, 138.41, 129.37, 124.44, 123.32, 122.91, 121.79, 79.25, 56.65, 56.11, 49.95, 42.30, 39.68, 39.49, 37.91, 36.81, 36.54, 36.16, 35.77, 31.89, 31.81, 28.21, 28.00, 27.62, 26.85, 24.27, 23.81, 22.81, 22.55, 21.03, 19.27, 18.70, 11.85.

**Data for 3b.** Mp 177 °C, IR (KBr)  $\nu_{\max}$  (cm<sup>-1</sup>) 2937, 2868, 2851, 1761, 1687, 1598, 1586, 1761, 1687, 1598, 1586, 1498, 1466, 1415, 1373, 1352, 1319, 1248, 1216, 1140, 1042, 1008, 951, 858, 849, 802; <sup>1</sup>H NMR (δ, CDCl<sub>3</sub>) 8.12 (d, *J* = 8.4 Hz, 2H), 8.03 (d, *J* = 7.7 Hz, 2H), 7.96 (d, *J* = 7.7 Hz, 2H), 7.37 (d, *J* = 8.8 Hz, 2H), 5.44 (d, *J* = 4.4 Hz, 1H), 4.59 (m, 1H), 3.07 (q, *J*<sub>1</sub> = 7.2 Hz, *J*<sub>2</sub> = 14.5 Hz, 2H), 2.51 (d, *J* = 7.2 Hz, 2H), 0.89–2.06 (m, 41H), 0.69 (s, 3H); <sup>13</sup>C (δ, CDCl<sub>3</sub>) 200.15, 154.80, 153.51, 152.44, 150.14, 139.03, 138.28, 129.02, 124.42, 123.33, 122.91, 121.79, 79.25, 56.67, 56.11, 49.97, 42.31, 39.69, 39.50, 37.91, 36.55, 36.16, 35.78, 32.10, 31.90, 31.83, 28.21, 28.01, 27.62, 24.27, 23.81, 22.81, 22.55, 21.04, 19.27, 18.70, 11.85, 8.20.

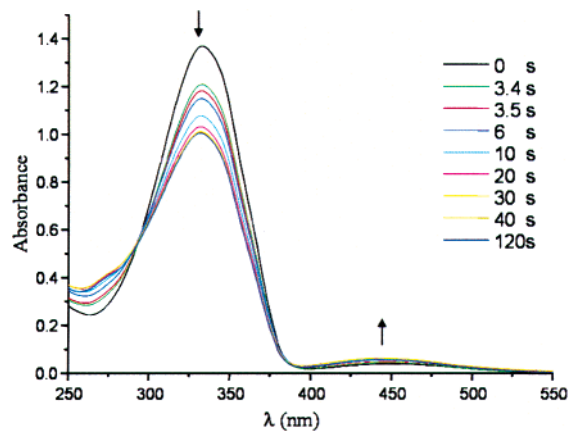
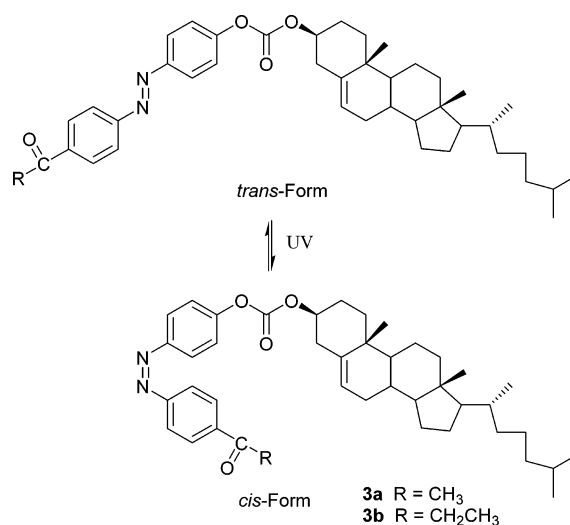


**Figure 1.** UV-vis absorption spectra of **3a** (50 μM) in CH<sub>2</sub>Cl<sub>2</sub> under irradiation (365 nm, at 0, 3.4, 3.5, 6, 10, 20, 30, 40, and 120 s).

### Scheme 2. UV-Induced *trans-cis* Isomerization of Azobenzene **3**



## Results and Discussion

Compounds **3a** and **3b** exhibited the expected reversible photoresponsive behavior (Scheme 2). For example, dark incubation of a dichloromethane solution (50 μM/mL) of **3a** has a maximum absorbance at 333 nm corresponding to the *trans*-azobenzene chromophore. Irradiation of this solution with 365 nm light resulted in photoisomerization to *cis*-**3a**, as evidenced by a decrease in the absorbance at 333 nm and an increase in absorbance at 439 nm. Also the absorbance at 266 nm appeared (Figure 1). The stationary population of *trans* and *cis* isomers is a function of irradiation intensity. A higher rate of photoisomerization transition is expected at a UV intensity higher than that applied in this work. Optical switching dynamics of compounds **3a** and **3b** were studied quantitatively by UV absorption measurements. Because the absorbance corresponding to *trans* and *cis* isomers is proportional to their population, we represent the population distribution on the two states by the absorption. Our experimental data agree well with eq 1, which shows that the population in the *trans* and *cis* states is an exponential function of time. This is consistent with other investigations.<sup>20</sup>

$$n = n_0(1 - ce^{-t/\tau}) \quad (1)$$

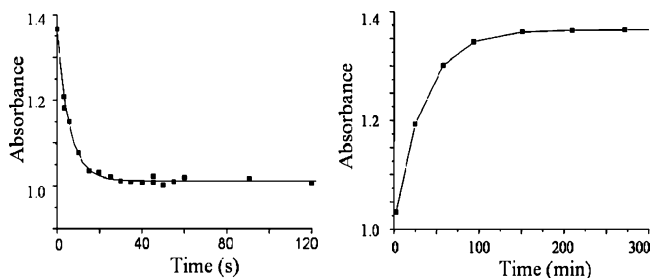


**Figure 2.** Left: plot of UV absorbance at 330 nm of **3a** in  $\text{CH}_2\text{Cl}_2$  under irradiation at 365 nm for different times. Right: plot of UV absorbance at 330 nm of **3a** in  $\text{CH}_2\text{Cl}_2$  in the dark at room temperature after irradiation of its solution with 365 nm of light resulting in photoisomerization to *cis*-**3a**.

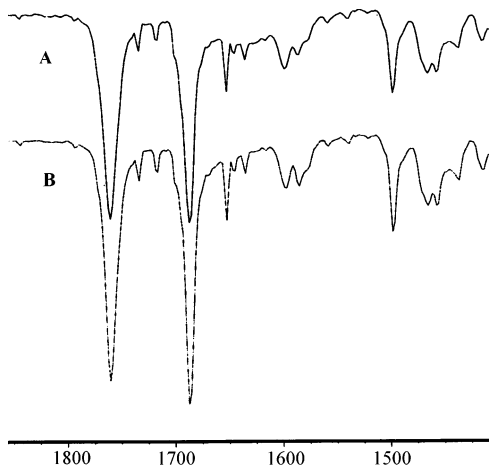


**Figure 3.** IR absorption band ( $\text{cm}^{-1}$ ) of **3b** (A, before irradiation at 365 nm; B, after irradiation at 365 nm for 30 min).

In eq 1,  $c$  is the coefficient proportional to excitation light intensity. A photostationary state from *trans*-**3a** to its *cis* isomer was reached within approximately 30 s under irradiation at 365 nm (Figure 2, left). Thermal reversion of *cis*-**3a** to its *trans* isomer is exhibited with a time constant of approximately 3 h at room temperature in the dark after an irradiation of the solution at 365 nm of light for 10 min (Figure 2, right). Ambient light can expedite this relaxation process by approximately one-third.

The reversible photo-induced conversion of the *trans* form to the *cis* form was observed by  $^1\text{H}$  NMR spectroscopy and IR spectroscopy as well. The acetyl group in *trans*-**3a** and *cis*-**3a** in  $\text{CDCl}_3$  appears as a singlet at  $\delta$  2.67 and 2.57, respectively. The changes of chemical shifts in the phenyl regions of the spectrum were also observed. When **3b** was irradiated by UV light (365 nm) for 30 min, some difference of its IR weak absorption band ( $\text{N}=\text{N}$ ) near the  $1585\text{ cm}^{-1}$  region was observed due to the configuration's change (Figure 3).

The two mesogenic moieties of cholesteryl and azobenzene with the unique polar carbonyl unit in the terminal chain in **3a** and **3b** promote liquid crystalline phase behavior, which was investigated by DSC and optical polarizing microscopy equipped with a temperature controller. Our preliminary results show that the compounds **3a** and **3b** have a sequence of very interesting mesophases besides the expected chiral

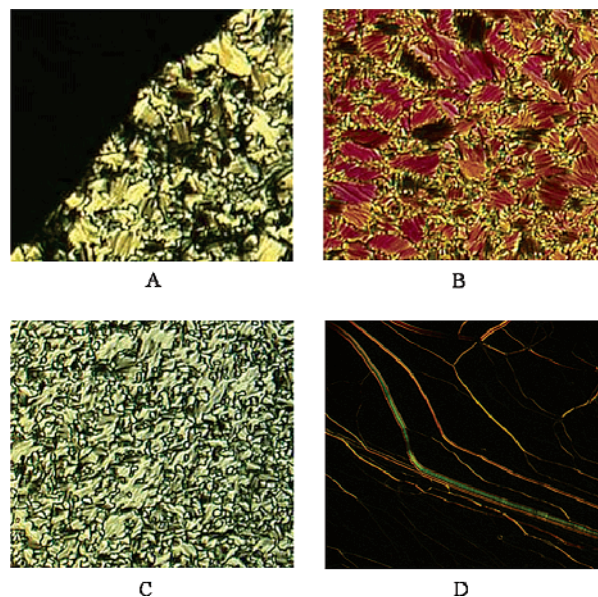
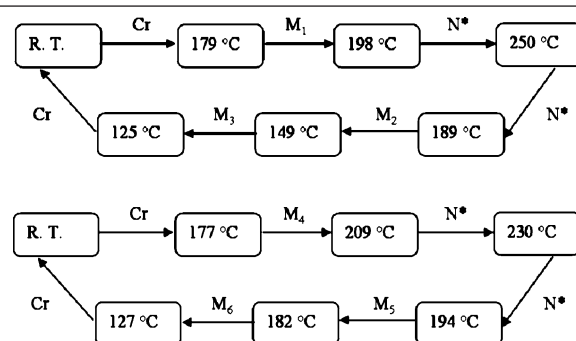


**Figure 4.** Crossed polarized optical texture micrograph of **3a** (A, B, and C on cooling at 149, 162, and 171  $^\circ\text{C}$ ; D on heating at 205  $^\circ\text{C}$ ; magnification  $\times 200$ ).

**Table 1.** Observed Phase Behavior for **3a** and **3b**<sup>a</sup>



<sup>a</sup> R.T. = room temperature, Cr = crystalline, M = mesophase to be identified,  $N^*$  = chiral nematic phase.

nematic mesophase with a characteristic oily streak texture (e.g., Figure 4D). The observed phase behavior for **3a** and **3b** is shown in Table 1. The materials **3a** and **3b** are thermally stable below 250 and 230  $^\circ\text{C}$ , respectively. Their chiral nematic phase was maintained until they started to decompose around 250 or 230  $^\circ\text{C}$ . We observed that an unidentified mesophase occurred below the  $M_3$  with isotropic optical property, showing up under the polarized microscope as completely black. As is shown in Figure 4A, the frontier of this phase propagates across the viewing scope of the microscope. This phenomenon has been seen in some banana-shape liquid crystals, and its structure is not yet fully understood in that system.<sup>21,22</sup> Interestingly, our synthetic molecule with *trans* configuration appears to have a banana shape (Figure 5). The chiral nature of the molecule makes it very possible to form a twisted structure while it is in a layered smectic phase; a TGB phase can be expected within a small temperature interval at the transition from nematic\* or smectic\*. With the current data obtained, we observed

(21) Pelzl, G.; Diele, S.; Weissflog, W. *Adv. Mater.* **1999**, *11*, 707.

(22) (a) Jakli, A.; Huang, Y.-M.; Fodor-Csorba, K.; Vajda, A.; Gallii, G.; Diele, S.; Pelzl, G. *Adv. Mater.* **2003**, *15*, 1606. (b) DiDonna, B. A.; Kamien, R. D. *Phys. Rev. Lett.* **2002**, *89*, 215504.

(20) Hogan, P. M.; Tajbakhsh, A. R.; Terentjev, E. M. *Phys. Rev. E* **2002**, *65*, 041720.



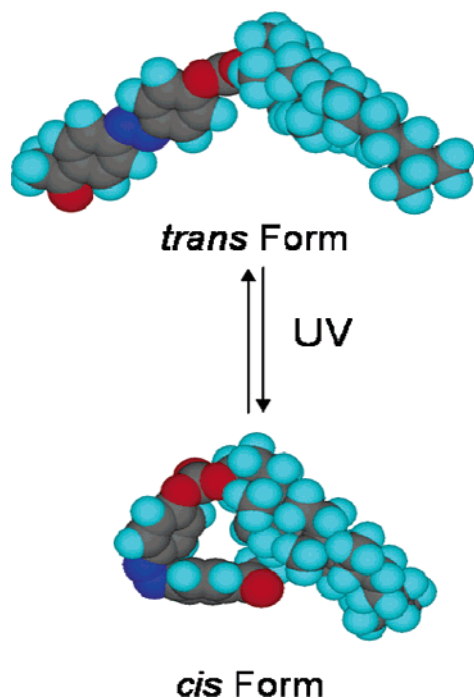


**Figure 5.** Space filling model of **3a** by 3D-ChemDraw.

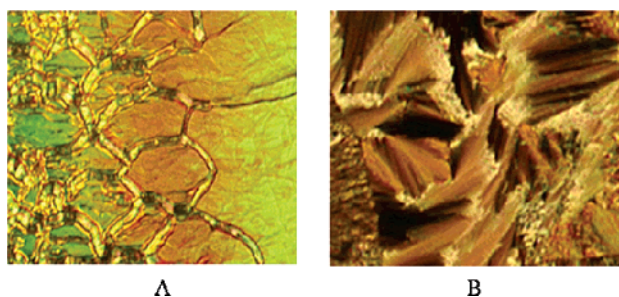


**Figure 6.** Crossed polarized optical texture micrograph of **3b** (A, heating at 209 °C; B, on cooling at 171 °C; magnification  $\times 200$ ).

that the crossed polarized optical textures resemble that of the TGBA\* phase (Figure 6). The phase sequence depends on their thermohistory and optical irradiation condition as well.

In the meantime, we used the compound **3b** as a chiral dye dopant to conventional nematic liquid crystal 5CB (achiral N–I transition at 35 °C); at the composition of 25% **3b** in 5CB, the mixture is homogeneously mixed and undergoes a chiral N–I transition temperature at 39.9 °C. The sample was capillary-filled into a thin glass cell (made in a 1000 clean room, with indium tin oxide coated glass substrates, with a cell gap of 16  $\mu\text{m}$ ) to form a 16  $\mu\text{m}$  thin film and placed on a Linkam heat stage that can control the sample temperature within 0.1 °C. A cholesteric polygonal fingerprint texture was observed at 38.9 °C, as shown in Figure 7A. UV irradiation at 365 nm was administered by a UV gun (10 mW/cm<sup>2</sup>, for polymer curing purpose) at the sample. Within 10 s under irradiation this sample transitions

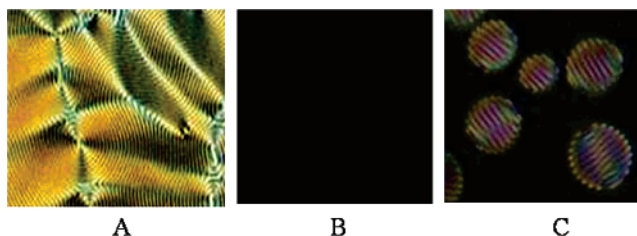


**Figure 7.** Crossed polarized optical texture micrograph of the mixture of 25% **3b** in 5CB on cooling at 38.9 °C (A, before UV irradiation; B, after UV irradiation for 10 s; C, 20 s after removal of UV light at the isotropic phase).

to the isotropic phase as evidenced by a texture change as shown in Figure 7B. It is shown by this experiment that the conversion from the trans to the cis configuration of the dopant leads to destabilization of the liquid crystalline phase of the mixture. Removal of UV light immediately leads to the reverse process of N\* domain formation from the isotropic phase appearing as droplet nucleation followed by coalescence (Figure 7C). The reversion to the original polygonal fingerprint texture in Figure 7A was reached within approximately 2 h at room temperature in the dark. This time scale is consistent with photoswitching dynamics measured by UV absorption. It is to be noted, however, that the almost immediate appearance of the N\* islands in the isotropic phase is a sensitive response of the destabilizing *cis* isomer of the dopant. A change in the *cis*-component concentration can induce a dramatic change in the mesophase stability. The further characterization of the interesting mesophases and investigation of their electrooptical properties are in progress.

## Conclusions

We synthesized two chiral liquid crystals for reversible photoresponsive properties were well-demonstrated. The chiral structure, UV tunable absorption at visible wavelength (440 nm), and liquid crystalline phase behavior make them potential display industry materials, as a chiral mesogenic dye dopant, in that they are compatible with other liquid crystals used in the liquid crystal display industry. Specifically, they have a very large solubility in a common nematic liquid crystal host, which can facilitate a large amount of doping to induce mesophase chirality and magnify the photocontrol effect. Their photoisomerization makes them promising candidates for chiral photochemical molecular switches and so forth.

**Acknowledgment.** This work is supported by LCI, KSU, and Ohio Board of Regents under its Research Challenge program. We gratefully thank Prof. O. Lavrentovich for the use of his characterization equipment and Prof. S. Kumar and Prof. Antal Jakli for fruitful discussions.

CM051404Z